is much smaller than those observed in the photoreduction of carbonyl molecules.[6,9] Thus, the effect due to the HF coupling mechanism is considered to be too small to be detected in the present reaction in spite of the large HF coupling constant of P (36.5 mT). The decrease in the decay rate of the $A(t)$ curve observed above 0.1 T in the present study can be explained by a relaxation mechanism[12] as shown in the following paragraph.

The $A(t)$ curves observed in the time range t = 70 ns to 9 μs in the absence and presence of a magnetic field of 1.2 T could be analyzed well by sets of two and three exponential functions, respectively. The results of the analysis using the method of least squares are shown in Figure 3 and by the following equations:

at 0 T

$$A(t') = 0.8923 \exp(-t'/139 \text{ ns}) + 0.1077 \exp(-t'/75\ \mu\text{s}) \quad (1)$$

at 1.2 T

$$A(t') = 0.7296 \exp(-t'/160 \text{ ns}) + 0.1498 \exp(-t'/677 \text{ ns}) + 0.1206 \exp(-t'/100\ \mu\text{s}) \quad (2)$$

Here, $t' = t - 70$ ns. Because the S/N ratios of the nearly constant components with lifetimes of 75 and 100 μs, respectively, are very small, the magnetic field effect on these components is considered to lie within the experimental errors. However, an extra decay component with a lifetime of about 680 ns appeared at 1.2 T for the decay of the radical pair other than the decay with a lifetime of about 160 ns. Such an extra component could not be observed at 0 T, where the decay of the radical pair can well be represented by an exponential function with a lifetime of about 140 ns. The appearance of the second decay component upon application of a magnetic field is characteristic of a magnetic field effect due to a relaxation mechanism in the case when a radical pair is prepared from a triplet precursor.[12]

Thus, the radical pair produced in the photodecomposition of TMDPO in an SDS micelle can be shown to be prepared more efficiently from the triplet state of TMDPO than from its singlet excited states. Sumiyoshi et al. estimated the lifetime of triplet TMDPO as 0.3 ns.[11] Indeed, such a triplet state is considered to be too short-lived to be detected with conventional nanosecond-laser flash photolysis techniques.

The second decay component observed in the presence of a magnetic field originates from the relaxation from the $T_{\pm 1}$ levels of a radical pair to its T_0 and S levels.[12] Thus, for the present reaction, such an extra component was found to be induced by a magnetic field. From an analysis of the ^{31}P HF coupling tensor of the diphenylphosphonyl radical trapped in a single crystal,[13] the 3s and 3p characters of ^{31}P were obtained to be 0.11 and 0.60, respectively. Thus, the odd electron of this radical was found to be nearly localized on ^{31}P. Therefore, in the present study, we could observe an appreciable magnetic field effect on the rate of reaction between phosphorus- and carbon-centered radicals with the laser flash photolysis technique.

(12) Hayashi, H.; Nagakura, S. *Bull. Chem. Soc. Jpn.* **1984**, *57*, 322.

(13) Geoffroy, M.; Lucken, E. A. C. *Mol. Phys.* **1971**, *22*, 257.

Adiabatic vs. Nonadiabatic Electron Transfer and Longitudinal Solvent Dielectric Relaxation: Beyond the Debye Model

Massimo Sparpaglione and Shaul Mukamel*†

Department of Chemistry, University of Rochester, Rochester, New York 14627 *(Received: April 29, 1987)*

A theory for electron-transfer rates in a polar medium is developed using an expansion of the density matrix in Liouville space and utilizing the analogy with the problem of nonlinear optical line shapes. A separation of time scales between the populations and coherences (diagonal and off-diagonal elements of the density matrix, respectively) allows us to carry an approximate summation of the rate to infinite order in the nonadiabatic coupling. A closed expression for the rate and a novel criterion for adiabaticity, involving the entire frequency and wavevector-dependent dielectric function of the solvent $\epsilon(\mathbf{k},\omega)$ are derived. A proper definition of the relevant solvent time scale in terms of $\epsilon(\mathbf{k},\omega)$, which is not restricted to the Debye model, is obtained. The role of the solvent longitudinal dielectric relaxation in inducing the crossover from the nonadiabatic to the adiabatic regimes is analyzed.

I. Introduction

The effects of solvation dynamics and relaxation on the rates of electron-transfer (ET) processes had received considerable attention recently.[1-5] It has long been recognized that the ET rate is usually controlled by the dynamics of dielectric fluctuations in the surrounding medium (the solvent).[6-8] Favorable fluctuations, which make the initial and the final states temporarily isoenergetic, are crucial in inducing the electron transfer. The theory of Marcus[6] uses a classical dielectric continuum formulation to express the rate to second-order perturbation theory in the electronic coupling matrix element V between the initial and the final states. This theory had remarkable success in predicting the electron-transfer rate in terms of the static and the high-frequency dielectric constants of the solvent (ϵ_0 and ϵ_∞, respectively). A parabolic dependence of the logarithm of the reaction rate (the activation free energy) on the exothermicity has been predicted and confirmed.[9] As the coupling matrix element V increases, this perturbative expression in V will no longer be valid. It is expected that for large V, or when the solvent motions are suf-

† Camille and Henry Dreyfus Teacher-Scholar.

(1) Kosower, E. M. *Acc. Chem. Res.* **1982**, *15*, 259; *J. Am. Chem. Soc.* **1985**, *107*, 1114. Kosower, E. M.; Huppert, D. *Chem. Phys. Lett.* **1983**, *96*, 423. Kosower, E. M.; Huppert, D. *Annu. Rev. Phys. Chem.* **1986**, *37*, 127.

(2) Wang, Y.; Eisenthal, K. B. *J. Chem. Phys.* **1982**, *77*, 6067. Millar, D. P.; Eisenthal, K. B. *J. Chem. Phys.* **1985**, *83*, 5076.

(3) Heisel, F.; Miehe, J. A. *Chem. Phys.* **1985**, *98*, 233.

(4) Weaver, M. J.; Gennett, T. *Chem. Phys. Lett.* **1985**, *113*, 213.

(5) McGuire, M.; McLendon, G. *J. Phys. Chem.* **1986**, *90*, 2549.

(6) Marcus, R. A. *J. Chem. Phys.* **1956**, *24*, 966. For a review, see: Marcus, R. A. *Annu. Rev. Phys. Chem.* **1964**, *15*, 155. Sumi, H.; Marcus, R. A. *J. Chem. Phys.* **1986**, *84*, 4894.

(7) Levich, V. In *Physical Chemistry: An Advanced Treatise*; Eyring, H., Henderson, D., Jost, W., Eds.; Academic: New York, 1970; Vol. 9B. Dogonadze, R., In *The Chemical Physics of Solvation; Part A*; Dogonadze, R., Kalman, E., Kornyshev, A. A., Ulstrup, J., Eds.; Elsevier: Amsterdam, 1985; Vol. 1.

(8) Jortner, J.; Ulstrup, J. *J. Am. Chem. Soc.* **1979**, *101*, 3744. Redi, M. H.; Gerstman, B. S.; Hopfield, J. J. *Biophys. J.* **1981**, *35*, 471.

(9) Miller, J. R.; Calcaterra, L. T.; Closs, G. L. *J. Am. Chem. Soc.* **1984**, *106*, 3047.

0022-3654/87/2091-3938$01.50/0 © 1987 American Chemical Society

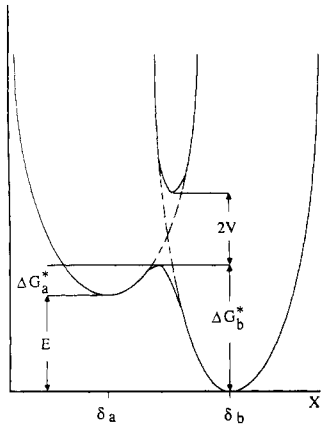

Figure 1. The free energy surface for electron transfer as a function of the solvation coordinate x. δ_a is the equilibrium value of x, and ΔG_a^* is the free energy of activation when the electron-transfer system is in state $|a\rangle$. δ_b and ΔG_b^* are the corresponding quantities when the system is in the state $|b\rangle$. V is the electronic coupling matrix element.

ficiently slow, the rate will become independent on V, and the nonadiabatic reaction will become adiabatic. In that limit the ET dynamics can be described by a motion on a single potential surface with a barrier. Kosower and Huppert[1] had demonstrated that adiabatic barrierless photochemical intramolecular electron-transfer rates in alcohols are correlated with the inverse solvent longitudinal relaxation time. The problem of adiabatic rate processes has been the subject of extensive studies following the pioneering work of Kramers,[10-15] who derived an expression for the effect of the solvent on the rate using a stochastic Langevin approach. Zusman[13] had developed a nonperturbative expression for the rate assuming that the solvent dielectric function is Lorentzian in frequency (the Debye model) and that the activation barrier is high.[16] His formulation cannot be easily generalized to barrierless reactions and to non-Debye solvents.

In this article we develop a theory for ET rates in polar solvents by utilizing the formal analogy of this problem with the calculation of nonlinear optical line shapes. The perturbative calculation of the rate (to order V^2) is formally equivalent to the calculation of ordinary spectral line shapes in a weak electromagnetic field. Similarly, the nonperturbative calculation of the rate and the transition to the adiabatic limit bear close formal resemblance to the problem of nonlinear optical line shapes. The transition to the adiabatic regime is strikingly analogous to the saturation of spectral line shapes in a strong radiation field (the Karplus–Schwinger line shape).[17,18] We have developed equations of motion for the density matrix in Liouville space which allow the calculation of spectral line shapes in nonlinear optical processes.[18-20] In this article, we use that formulation to derive a closed form expression for the electron-transfer rate in a polar solvent. The approach is based on projection operators in Liouville space,[21] followed by an approximate resummation of the perturbative series for the rate to infinite order in the electronic coupling V. Our final result is given in terms of the entire solvent dielectric function $\epsilon(\mathbf{k},\omega)$ and is not restricted to the Debye model. It interpolates between the adiabatic and the nonadiabatic limits and holds for high as well as low activation barriers. The effects of the solvent on the rate are analogous to the dephasing processes which dominate the optical spectral line shapes. In section II, we introduce the solvation coordinate and present a general expression for the rate (eq 3) in terms of an ordinary line-shape function $\sigma(E)$, the equilibrium distribution of the solvation coordinate $S_j(E)$, and a solvent characteristic time $\tau_{s,j}(E)$, j = a, b. Here $|a\rangle$ and $|b\rangle$ denote the initial and the final states for the electron-transfer process (Figure 1). These quantities are then related to the wavevector and frequency-dependent dielectric function of the solvent $\epsilon(\mathbf{k},\omega)$. A unified criterion for adiabaticity (eq 17), which is not restricted to high activation barriers, is obtained. In section III, we apply these results to the Debye model of ϵ and derive an explicit expression for the rate in terms of ϵ_0, ϵ_∞, and the longitudinal relaxation time τ_L. Numerical calculations show the Kramers turnover regime as well as the Marcus free energy curve. These results are summarized and discussed in section IV.

II. The Solvation Coordinate and the Electron-Transfer Rate

We consider an electron-transfer process between two molecules in a polar solvent. We denote the electronic state of the system when the electron is on the donor and the acceptor by $|a\rangle$ and $|b\rangle$, respectively. The Hamiltonian of the system is

$$H = |a\rangle H_a\langle a| + |b\rangle(H_b - E)\langle b| + V(|a\rangle\langle b| + |b\rangle\langle a|) \quad (1)$$

Here H_a and H_b are the solvent Hamiltonians when the charge-transfer system is in the states $|a\rangle$ and $|b\rangle$, respectively. E is the exothermicity of the reaction. We assume that initially the system is in the state $|a\rangle$, and we shall be interested in calculating the rate constant K for electron transfer to state $|b\rangle$. The solvation coordinate U is defined as

$$U \equiv H_b - H_a = -\int \mathbf{dr}\,[D_b(\mathbf{r}) - D_a(\mathbf{r})]P(\mathbf{r}) \quad (2)$$

Here $D_a(\mathbf{r})$ and $D_b(\mathbf{r})$ is the electric field, at point $\mathbf{r}$, produced by the static charge distribution of the donor and acceptor in the states $|a\rangle$ and $|b\rangle$, respectively, $P(\mathbf{r})$ is the polarization of the solvent at the point $\mathbf{r}$.

The calculation of the rate was carried out using an expansion of the density matrix in Liouville space.[18-21] It is assumed that the only dynamical variable of the solvent relevant for the electron transfer is the solvation coordinate (eq 2). A projection operator is then constructed which projects the complete solvent dynamics into that of the solvation coordinate, and the ET rate is expanded in a power series in V. An approximate infinite resummation of this series, analogous to the calculation of nonlinear optical line shapes, is then carried out. The resummation makes use of the separation of time scales between the off-diagonal elements, which undergo rapid dephasing, and the diagonal elements which survive for longer times. The final expression for the ET rate is[22]

$$K = \frac{2\pi(V^2/\hbar)\sigma(\delta_a - E)}{1 + 2\pi(V^2/\hbar)[S_a(E) + S_b(E)]\tau_s} \quad (3)$$

with

$$\tau_s = \frac{S_a(E)\tau_{s,a} + S_b(E)\tau_{s,b}}{S_a(E) + S_b(E)} \quad (4)$$

Here $\sigma(E)$ is an ordinary absorption line-shape function for the $|a\rangle$ to $|b\rangle$ electronic transition, $S_a(E)$ is the probability of the solvation coordinate to have the value E at equilibrium when the electron is in the $|a\rangle$ state, whereas $\tau_{s,a}$ is a characteristic solvent relaxation time when the electron is in state $|a\rangle$ and the solvent is perturbed around configurations with energy $E - \delta_a$. $S_b(E)$ and $\tau_{s,b}$ are the corresponding quantities when the charge-transfer system is in the state $|b\rangle$. τ_s is an averaged solvent relaxation time which is relevant for the dynamics of the ET process and controls

(10) Kramers, H. A. *Physica* **1940**, *7*, 284.
(11) Schroeder, J.; Troe, J. *Chem. Phys. Lett.* **1985**, *116*, 453. Maneke, G.; Schroeder, J.; Troe, J.; Voss, F. *Ber. Bunsenges. Phys. Chem.* **1985**, *89*, 896. Lee, M.; Holton, G. R.; Hochstrasser, R. M. *Chem. Phys. Lett.* **1985**, *118*, 359.
(12) Rothenberger, G.; Negus, D. K.; Hochstrasser, R. M. *J. Chem. Phys.* **1983**, *79*, 5360. Velsko, S. P.; Waldeck, D. H.; Fleming, G. R. *J. Chem. Phys.* **1983**, *78*, 294. Bagchi, B.; Fleming, G. R.; Oxtoby, D. W. *J. Chem. Phys.* **1983**, *78*, 7375.
(13) Zusman, L. D. *Chem. Phys.* **1980**, *49*, 295.
(14) Grote, R. F.; Hynes, J. T. *J. Chem. Phys.* **1980**, *73*, 2715.
(15) Frauenfelder, H.; Wolynes, P. G. *Science* **1985**, *229*, 337.
(16) Fröhlich, H. *Theory of Dielectrics*; Oxford University Press: London, 1949.
(17) Karplus, R.; Schwinger, J. *Phys. Rev.* **1948**, *73*, 1020.
(18) Mukamel, S. *Phys. Rep.* **1982**, *93*, 1; *J. Chem. Phys.* **1980**, *73*, 5322.
(19) Sue, J.; Yan, Y. J.; Mukamel, S. *J. Chem. Phys.* **1986**, *85*, 462. Mukamel, S. *Adv Chem. Phys.*, in press.
(20) Loring, R. F.; Yan, Y. J.; Mukamel, S. *J. Chem. Phys.*, in press. Loring, R. F.; Mukamel, S. *J. Opt. Soc. Am. B* **1986**, *3*, 595.
(21) Abe, S.; Mukamel, S. *J. Chem. Phys.* **1983**, *79*, 5457.
(22) Sparpaglione, M.; Mukamel, S., to be published.

its adiabaticity. Assuming that the solvation coordinate U is a Gaussian process and making use of the second-order cumulant expansion, we obtain the following expressions for these dynamical quantities:

$$\sigma(x) = \frac{1}{\pi} \mathrm{Re} \int_0^\infty dt \exp[(i/\hbar)xt - g(t)] \tag{5}$$

with

$$g(t) = \Delta_a^2 \mathrm{Re} \int_0^t d\tau_1 \int_0^{\tau_1} d\tau_2 M_a(\tau_2) \tag{6a}$$

and

$$\delta_j = \langle U\rho_j \rangle \tag{6b}$$

$$\Delta_j^2 = \langle U^2\rho_j \rangle - \langle U\rho_j \rangle^2 \tag{6c}$$

$$\Delta_j^2 M_j(t) \equiv \langle \exp(iH_jt)U \exp(-iH_jt)U\rho_j \rangle - \langle U\rho_j \rangle^2, \quad j = a, b \tag{6d}$$

Here ρ_j is the equilibrium density matrix of the solvent, when the system is in the state $|j\rangle$, and the angular brackets $\langle ... \rangle$ denote a trace over the solvent degrees of freedom. Note that $M_j(0) = 1$. We further have

$$S_j(x) = \frac{1}{(2\pi)^{1/2}\Delta_j} \exp\left[-\frac{(x - \delta_j)^2}{2\Delta_j^2} \right] \tag{7}$$

$$\tau_{s,j} = \int_0^\infty dt \, [R_j(E,t;E) - 1] \tag{8}$$

with

$$R_j(x,t;x') = \frac{1}{(1 - M_j^2(t))^{1/2}} \exp\{-[(x - \delta_j)^2 + (x' - \delta_j)^2(2M_j^2(t) - 1) - 2M_j(t)(x - \delta_j)(x' - \delta_j)]/[2\Delta_j^2[1 - M_j^2(t))]\} \tag{9a}$$

and

$$R_j(E,t;E) = \frac{1}{(1 - M_j^2(t))^{1/2}} \exp\left[\frac{M_j(t)(E - \delta_j)^2}{\Delta_j^2[1 + M_j(t)]} \right] \tag{9b}$$

Here $R_j(x,t;x')S_j(x')$ is the conditional probability for the solvation coordinate to have the value x at time t given that it had the value x' at $t = 0$, and that the molecular system is in state $|j\rangle$, j = a, b. Note that $\tau_{s,j}$ depends only on the diagonal part of R_j, i.e., $R_j(E,t;E)$. $\tau_{s,j}$ can be interpreted as a typical time scale for the solvation coordinate to relax when it is perturbed around $x = E$ and the electron is in state $|j\rangle$. In eq 3–9, the effects of the solvent enter in the shifts δ_j, the variances Δ_j^2, and the correlation functions $M_j(t)$. Using perturbation theory in the solvent system interaction, we can express these quantities in terms of the dielectric function of the solvent $\epsilon(\mathbf{k},\omega)$. Within this approximation, Δ_j and M_j are independent of j, and we shall omit the subscript j. We then get

$$\Delta^2 M(t) = \int\int d\mathbf{r}_1 \, d\mathbf{r}_2 \, [D_a(\mathbf{r}_1) - D_b(\mathbf{r}_1)][D_a(\mathbf{r}_2) - D_b(\mathbf{r}_2)]C_{PP}(\mathbf{r}_1 - \mathbf{r}_2, t) \tag{10a}$$

$$\delta_j = -\int_0^{(k_BT)^{-1}} d\lambda \int\int d\mathbf{r}_1 \, d\mathbf{r}_2 \, [D_a(\mathbf{r}_1) - D_b(\mathbf{r}_1)] \cdot D_j(\mathbf{r}_2)C_{PP}(\mathbf{r}_1 - \mathbf{r}_2, -i\lambda) \tag{10b}$$

where

$$C_{PP}(\mathbf{r}_1 - \mathbf{r}_2, t) \equiv \langle P(\mathbf{r}_1,t) \, P(\mathbf{r}_2,0) \rangle = \frac{ik_BT}{2(2\pi)^5} \int_{-\infty}^{\infty} d\mathbf{k} \int_{-\infty}^{\infty} \frac{d\omega}{\omega} \exp[-i\omega t - i\mathbf{k}(\mathbf{r}_1 - \mathbf{r}_2)] \times \left[\frac{1}{\epsilon(\mathbf{k},0)} - \frac{1}{\epsilon(\mathbf{k},\omega)} \right] \tag{10c}$$

Here $D_j(r)$ is the electric field produced by the static charge distribution of the system in state $|j\rangle$, Δ^2 equal to the right-hand side of eq 10a at $t = 0$, so that $M(0) = 1$. $C_{PP}(\mathbf{r},t)$ is the equilibrium correlation function of the solvent polarization, which is related to its dielectric function.

Equations 10 relate the electron-transfer rate to the wavevector and frequency-dependent dielectric function of the solvent $\epsilon(\mathbf{k},\omega)$. Usually, only the long wavelength ($\mathbf{k} = 0$) component of ϵ is known experimentally.[23] A procedure by which $\epsilon(0,\omega)$ may be used to obtain $\epsilon(\mathbf{k},\omega)$ for polar fluids was developed.[24] Using that procedure, we may then evaluate all the relevant quantities (eq 10), using $\epsilon(0,\omega)$. Hereafter, we assume that ϵ is independent of $\mathbf{k}$ and set

$$\epsilon(\mathbf{k},\omega) = \epsilon(0,\omega) \tag{11}$$

upon the substitution of eq 11 in eq 10c, we get

$$C_{PP}(\mathbf{r}_1 - \mathbf{r}_2, t) = \frac{ik_BT}{8\pi^2} \delta(\mathbf{r}_1 - \mathbf{r}_2) \int_{-\infty}^{+\infty} \frac{d\omega}{\omega} \exp(-i\omega t) \left[\frac{1}{\epsilon(0,0)} - \frac{1}{\epsilon(0,\omega)} \right] \tag{12}$$

Making use of eq 10–12, we can express all the dynamical quantities appearing in the rate (eq 3) in terms of $\epsilon(0,\omega)$; i.e.

$$S_j(E) = \frac{1}{(2\pi)^{1/2}\Delta} \exp\left[-\frac{(E - \delta_j)^2}{2\Delta^2} \right] \tag{13}$$

$$\delta_j = -\frac{i}{8\pi^2} \int d\mathbf{r} \, [D_a(\mathbf{r}) - D_b(\mathbf{r})]D_j(\mathbf{r}) \int \frac{d\omega}{\omega} \left[\frac{1}{\epsilon(0,0)} - \frac{1}{\epsilon(0,\omega)} \right] \tag{14a}$$

$$\Delta^2 = k_BT|\delta_a - \delta_b| \tag{14b}$$

$$Q(t) = \int_{-\infty}^{\infty} \frac{d\omega}{\omega} \exp(-i\omega t) \left[\frac{1}{\epsilon(0,0)} - \frac{1}{\epsilon(0,\omega)} \right] \tag{15a}$$

$$M(t) = Q(t)/Q(0) \tag{15b}$$

The line-shape function σ is given by eq 5 with $\Delta_a = \Delta$ and $M_a(t) = M(t)$. We further have

$$\tau_{s,j} = \exp(q_j^2/2) \, \tau(q_j) \qquad j = a, b \tag{16a}$$

with

$$\tau(q_j) \equiv \exp(-q_j^2/2) \int_0^\infty dt \left\{ \frac{1}{(1 - M^2(t))^{1/2}} \exp\left[\frac{q_j^2 M(t)}{1 + M(t)} \right] - 1 \right\} \tag{16b}$$

and

$$q_j \equiv \frac{E - \delta_j}{(k_BT|\delta_a - \delta_b|)^{1/2}} \tag{16c}$$

$\tau(q_j)$ is a characteristic relaxation time for the solvent fluctuations when the solvation coordinate is perturbed around $x = E - \delta_j = (k_BT|\delta_a - \delta_b|)^{1/2}q_j$.

Equation 3 provides us with a novel criterion for adiabaticity. We introduce the adiabaticity parameter

$$\nu \equiv (V^2/\hbar)[S_a(E) + S_b(E)]\tau_s \tag{17}$$

When ν is small, the reaction is nonadiabatic, and the rate is proportional to V^2; i.e.

$$K = (V^2/\hbar)\sigma(\delta_a - E) \qquad \nu \ll 1 \tag{18a}$$

In the other extreme, the rate is independent on V, and we get

$$K = \frac{\sigma(\delta_a - E)}{S_a(E) + S_b(E)} \frac{1}{\tau_s} \qquad \nu \gg 1 \tag{18b}$$

τ_s is, therefore, the characteristic solvent time scale which controls the adiabaticity of the ET process. An ET process which is

(23) Bottcher, C. J. F.; Bordewijk, P. *Theory of Electric Polarization*; Elsevier: Amsterdam, 1978; Vol. 2.
(24) Loring, R. F.; Mukamel, S. *J. Chem. Phys.*, in press.

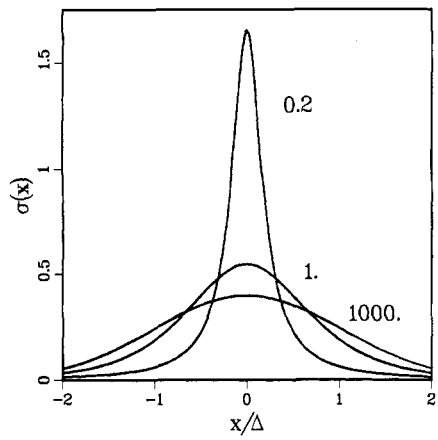

Figure 2. The line-shape function $\sigma(x)$ for the Debye model is displayed for different values of the longitudinal relaxation time τ_L. Each curve is labeled by the corresponding relaxation time τ_L, given in units of $\hbar/\Delta$. The coordinate x is given in units of Δ. As τ_L increases $\sigma(x)$ changes from a Lorentzian to a Gaussian.

nonadiabatic for small τ_s will eventually become adiabatic as τ_s is increased. The precise definition of τ_s (eq 4 and 16) is one of the major results of this article.

III. Application to the Debye Model

Equation 3 provides an expression for the ET rate for a solvent with an arbitrary dielectric function $\epsilon(0,\omega)$. We shall now analyze it for the Debye model;[16,23] i.e.

$$\epsilon(0,\omega) = \epsilon_\infty + (\epsilon_0 - \epsilon_\infty)/(1 - i\omega\tau_D) \tag{19}$$

where τ_D is the Debye relaxation time. Using eq 12 and 13, we then get

$$\delta_j = (4\pi)^{-1}[1/\epsilon_0 - 1/\epsilon_\infty]\int \mathbf{dr}\ [D_a(\mathbf{r}) - D_b(\mathbf{r})]D_j(\mathbf{r}) \tag{20a}$$

$$M(t) = \exp(-t/\tau_L) \tag{20b}$$

where the longitudinal dielectric relaxation time is

$$\tau_L \equiv (\epsilon_\infty/\epsilon_0)\tau_D \tag{20c}$$

and Δ^2 is given by eq 10a. We shall start our analysis with the nonadiabatic rate (eq 18a). The line-shape function $\sigma(x)$, (eq 5), has a maximum at $x = 0$. Near the line center for $x \ll \hbar/\tau_L$, the line shape assumes a Lorentzian form[19]

$$\sigma(x) = \frac{k_BT|\delta_a - \delta_b|\tau_L/(\pi\hbar)}{x^2 + [k_BT|\delta_a - \delta_b|\tau_L/\hbar]^2} \tag{21a}$$

In the wings, i.e., $x \gg \hbar/\tau_L$, the line shape is Gaussian

$$\sigma(x) = \frac{1}{(2\pi k_BT|\delta_a - \delta_b|)^{1/2}}\exp[-x^2/(2k_BT|\delta_a - \delta_b|)] \tag{21b}$$

The full width at half-maximum of the line shape $\sigma(x)$ is[19]

$$\Gamma_0 = (k_BT|\delta_a - \delta_b|)^{1/2}\frac{2.335 + 1.76\kappa}{1 + 0.85\kappa + 0.88\kappa^2} \tag{22}$$

The line shape $\sigma(x)$ is dominated by the parameter

$$\kappa = \frac{\hbar}{\Delta\tau_L} = \frac{\hbar}{(k_BT|\delta_a - \delta_b|)^{1/2}\tau_L} \tag{23}$$

The following conclusions may be obtained by a close examination of eq 20–23. For $\kappa \gg 1$ the line shape is Lorentzian over many widths since $\Gamma_0 \ll \hbar/\tau_L$. For $\kappa \ll 1$ the line is Gaussian since $\Gamma_0 \gg \hbar/\tau_L$, and the onset of Gaussian behavior occurs near the line center. In Figure 2 we show $\sigma(x)$ for various values of τ_L (as indicated). The transition from Lorentzian to Gaussian as τ_L increases is clearly demonstrated.

Equation 18a together with eq 21–23 allow us to predict the variation of the nonadiabatic rate with τ_L. Suppose we start with a very short τ_L. In this case the line shape $\sigma(x)$ will be a very narrow Lorentzian (motional narrowing) and assuming that $|E$

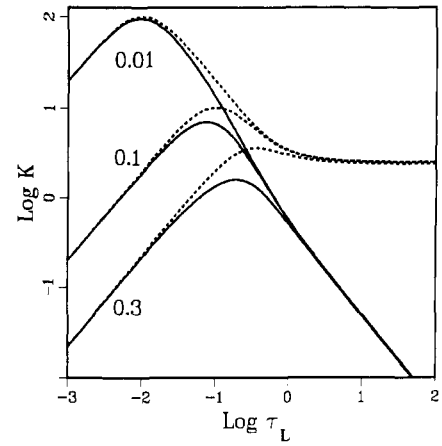

Figure 3. The ET rate vs. the longitudinal relaxation time for small barriers. The solid lines represent our result (eq 3) for $\Delta = 1$, $V = 1$, $\delta_a = 1$, $\delta_b = 2$. Each curve is labeled by the value of the exothermicity E. The dashed curves are the nonadiabatic rates (eq 18a), shown for comparison. For small τ_L the nonadiabatic limit holds, and the rate is proportional to τ_L. As τ_L increases, the nonadiabatic rate assumes a constant value independent of τ_L, whereas the complete expression (eq 3) decreases as $1/\tau_L$. The solid lines clearly show the Kramers turnover regime. τ_L is given in units of $\hbar/\Delta$.

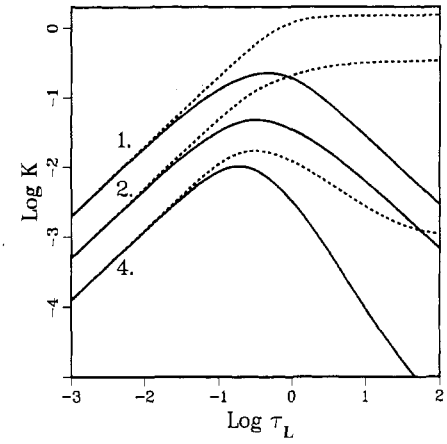

Figure 4. The same as Figure 4 but for larger values of the exothermicity (as indicated), corresponding to larger activation barriers.

$- \delta_a|$ is finite, the rate will be given by eq 21a where x is in the line wings $x \gg k_BT|\delta_a - \delta_b|\tau_L$. Under these circumstances K will grow $\sim\tau_L$. As τ_L is increased further, the line shape will remain a Lorentzian but with a larger width ($\sim\tau_L$). When $x < k_BT|\delta_a - \delta_b|\tau_L$, the rate will be given by eq 21a at the center ($x = 0$) and will decrease as τ_L^{-1}. When τ_L is increased even further, the line shape will eventually turn into a Gaussian (eq 21b) and the rate will become independent of τ_L. We thus have a crossover between three regimes: the wings of a Lorentzian for very short τ_L, the center of a Lorentzian for intermediate τ_L, and the Gaussian for large τ_L. The rate when plotted vs. τ_L will show a maximum and then reach a plateau. This behavior is illustrated by the dashed curves in Figures 3 and 4.

We shall now consider the transition to the adiabatic regime whereby the rate (eq 3) gradually attains the limiting form (eq 18b) with the solvent time scale τ_s defined in eq 16, together with eq 20c. The function $\tau(q)$ (and consequently τ_s) is proportional to τ_L. In Figure 5, we display $\tau(q)/\tau_L$ vs. q. The behavior of $\tau(q)$ for small and for large q can be found analytically, i.e.

$$\tau(q) = \left[\ln 2 + \left(1 - \frac{\ln 2}{2}\right)q^2\right]\tau_L \qquad q^2 \ll 2$$

$$= \frac{(2\pi)^{1/2}}{q}\tau_L \qquad q^2 \gg 2 \tag{24}$$

The dashed curve in Figure 5 shows the asymptotic form $(2\pi)^{1/2}/q$. Since $\tau(q)$ and the adiabaticity parameter ν (eq 17) are pro-

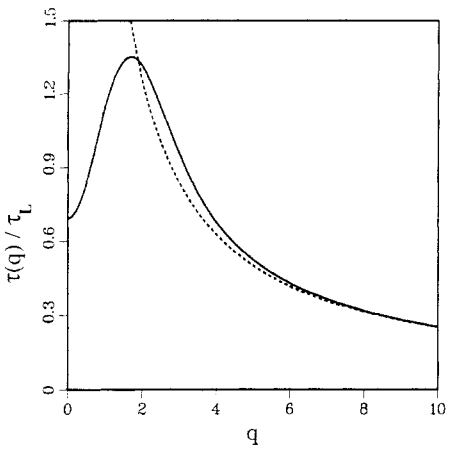

Figure 5. The function $\tau(q)$ (eq 16b), which controls the relevant solvent time scale τ_s and the adiabaticity parameter, is plotted vs. q for the Debye model. The solid line is the exact $\tau(q)/\tau_L$, calculated numerically. The dashed curve is the asymptotic form $\sim(2\pi)^{1/2}/q$, which holds for $q \gtrsim 2$.

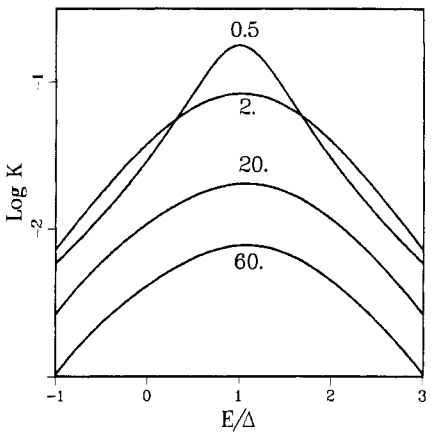

Figure 6. The logarithm of the rate (eq 3) is plotted against the exothermicity E. Each curve is labeled by the value of the longitudinal relaxation time. For $\tau_L = 0.5$ the reaction is nonadiabatic and it changes to adiabatic as τ_L is increased. Times are given in units of $\hbar/\Delta$ and energies in units of Δ. $V = 0.2$, $\delta_a = 1$, $\delta_b = 2$.

portional to τ_L, we predict that for large τ_L, the adiabatic rate will decrease as τ_L^{-1}. The plateau regime of the nonadiabatic rate (dashed curves in Figures 3 and 4) will thus turn into a $1/\tau_L$ behavior. The solid curves in Figures 3 and 4 show the τ_L dependence of the rate (eq 3). The maximum in the rate is the Kramers turnover.[10] Making use of eq 18b, together with eq 16 and eq 24, we can write a closed expression for the adiabatic rate. The line-shape function $\sigma(x)$ is taken to be Gaussian (eq 21b) and so is $S_j(x)$; i.e.,

$$S_j(E) = \frac{1}{(2\pi k_B T|\delta_a - \delta_b|)^{1/2}} \exp[-(E - \delta_j)^2/(2k_B T|\delta_a - \delta_b|)] \tag{25}$$

For high barriers $(E - \delta_a)^2/(k_B T|\delta_a - \delta_b|) > 2$, the adiabatic rate (eq 18b) thus assumes the form

$$K = \left(\frac{2\pi}{k_B T|\delta_a - \delta_b|}\right)^{1/2}\left[\frac{1}{|(E - \delta_a|} + \frac{1}{|E - \delta_b|}\right]^{-1}\frac{1}{\tau_L}\exp\left[-\frac{(E - \delta_a)^2}{2k_B T|\delta_a - \delta_b|}\right] \tag{26a}$$

In the opposite limit of low barriers $(E - \delta_a)^2/(k_B T|\delta_a - \delta_b| < 2$, and assuming further that the reverse reaction is very slow, $S_b(E) \ll S_a(E)$, we get

$$K = \frac{1}{\tau_s} = \frac{1}{a\tau_L} \tag{26b}$$

a is a constant order of 1. Its exact value is determined by the barrier height. For barrierless reactions, we have $a = \ln 2$. Finally in Figure 6, we display the rate (eq 3) as a function of the exothermicity E for various values of τ_L (as indicated). For small τ_L we recover the Marcus parabolic turnover. The figure demonstrates how this curve is modified as we cross into the adiabatic regime (large τ_L).

IV. Concluding Remarks

In conclusion, we shall summarize the main steps and results of this article. The present approach is based on the assumption that only a single collective solvent coordinate (the solvation coordinate U) is relevant for the dynamics of the ET process. The calculation of the rate was accomplished by formulating the dynamics in Liouville space using the density matrix of the ET system and the solvation coordinate. An approximate projection operator allows us to trace over all the other solvent degrees of freedom and focus on the solvation coordinate. In this way, the problem becomes analogous to the calculation of nonlinear optical line shapes.[18-21] When the rate is expanded in even powers of the electronic coupling V, the term $0(V^2)$ is analogous to ordinary (weak field) absorption line shape, whereas the term $0(V^4)$ is intimately related to the calculation of fluorescence, Raman, and four-wave mixing line shapes.[18-20] An approximate resummation of the perturbative series to infinite order in V was then performed, based on the assumption of separation of time scales between the off-diagonal density matrix elements (the coherences) and the diagonal elements (populations). The resulting expression (eq 3) interpolates between all the known limits of the rate and relates the activation free energy and the adiabaticity to the solvation dynamics. The activation free energy is determined by E, δ_j, and q_j, which are expected to be affected mainly by solvent polarity, whereas the solvent dynamics enter into the time scale function $\tau(q_j)$ through the polarization correlation function $M(t)$. Our expression satisfies properly the detailed balance condition, reproduces the entire Kramers turnover curve as a function of the solvent longitudinal time, interpolates continuously between the nonadiabatic and adiabatic limits, allows us to define the reaction free energy microscopically, and generalizes Marcus free energy relation to the nonadiabatic regime. An important issue, which is the subject of a current extensive debate,[1-6] is the precise definition of the solvent time scale relevant for the ET rate. The present theory shows that this is τ_s, (eq 4 and 16), which is determined by the correlation function $M(t)$ (eq 10). $M(t)$ may in turn be expressed in terms of the solvent longitudinal polarization correlation function $C_{PP}(\mathbf{r}_1-\mathbf{r}_2,t)$ (eq 10c). The latter is related to the full wavevector and frequency-dependent dielectric function of the solvent $\epsilon(\mathbf{k},\omega)$ (eq 10c). The steps required to predict the ET rate by using the dielectric properties of the solvent involve therefore getting C_{PP}, then $M(t)$, and finally τ_s. In the calculations presented here, we have assumed that $\epsilon(\mathbf{k},\omega)$ is independent of $\mathbf{k}$ (eq 11). Our general expression (eq 3), however, is not restricted to this limit. Dielectric relaxation experiments are usually done in the long-wavelength limit and result in the $k = 0$ component of $\epsilon(\mathbf{k},\omega)$.[23] A systematic procedure for constructing $\epsilon(\mathbf{k},\omega)$ for a polar fluid, using $\epsilon(\mathbf{k}=0,\omega)$ as an input, was developed recently[24] and can be used within the present theory (eq 10). Given $\epsilon(0,\omega)$, we obtain $M(t)$ via eq 15. Note that $M(t)$ is related to the Fourier decomposition of $1/\epsilon(0,\omega)$ and not of $\epsilon(0,\omega)$. Usually, experimental data of $\epsilon(0,\omega)$ are analyzed in terms of a correlation function $F(t)$ which is related to the Fourier decomposition of $\epsilon(0,\omega)$. A common practice is to interpret $\epsilon(0,\omega)$ in terms of a sum of a few components corresponding to different Debye relaxation times (e.g., alcohols). Other forms use continuous distributions of Debye times (e.g., the Cole Davidson form).[23] It should be emphasized that these Debye times are not the true longitudinal time scales of the solvent.[24] In general, if $F(t)$ is a superposition of N Debye relaxation functions with times t_j, $M(t)$ will also have N relaxation times t_j'. t_j' are however distinctly different from t_j. It is the latter time scales that are relevant for the ET rate. For the Debye model we have a single

relaxation time $t_1 = \tau_D$ and the longitudinal time $t_1' = \tau(0) = \ln 2\ \tau_L = \ln 2\ \tau_D(\epsilon_\infty/\epsilon_0)$. This relation holds only for the Debye model. In general we cannot go from t_j to t_j' by simply multiplying with $(\epsilon_\infty/\epsilon_0)$. The correct general procedure is to use $\epsilon(0,\omega)$ to get $M(t)$ which will subsequently yield t_j'. Finally, it should be noted that for small barriers, simple rate equations may not hold, and the ET process should be described by a generalized master equation with a memory (time-dependent rate $K(t)$). The present formulation is valid also in this case and provides an expression for $K(t)$. This will be analyzed in the future.

Acknowledgment. The support of the National Science Foundation, the Office of Naval Research, the US Army Research Office, and the donors of the Petroleum Research Fund, administered by the American Chemical Society, is gratefully acknowledged.

Preparation and Structure of Fully Cs^+-Exchanged Zeolite A

Nam Ho Heo, Chadin Dejsupa, and Karl Seff*

Chemistry Department, University of Hawaii, Honolulu, Hawaii 96822 *(Received: May 14, 1987)*

Fully Cs^+-exchanged zeolite A, a most ionically crowded zeolite A, has been prepared: Cs_{12}-A·$^1/_2$Cs by the reduction of Na^+ in dehydrated Na_{12}-A with cesium vapor ($\Delta E°_{aq} = +0.21$ V), and Cs_{12}-A·CsOH by the reaction of hydrated $(NH_4^+)_{12}$-A with cesium hydroxide ($K = 5.6 \times 10^4$). (These rational compositions differ insignificantly from those found experimentally.) Their structures ($a = 12.279$ (1) and 12.291 (5) Å, respectively) have been determined by single-crystal X-ray diffraction methods in the cubic space group $Pm3m$ with final R(weighted) indices of 0.042 and 0.093, respectively. In each structure, 2 Cs^+ ions are found about 4.05 Å apart in each sodalite unit, while 3 Cs^+ ions per unit cell are located in the centers of 8-rings. In Cs_{12}-A·$^1/_2$Cs, viewed as a mixture of Cs_{12}-A and Cs_{13}-A, 6 or 8 Cs^+ ions per unit cell lie opposite 6-rings in large cavity. The electrons of the excess Cs atoms have not delocalized to form a metallic continuum among Cs^+ ions with intercesium distances comparable to those in cesium metal. Rather they remain localized among the closest Cs^+ ions to give linear $(Cs_4)^{3+}$ cations. The hydroxide ion in Cs_{12}-A·CsOH is presumed to be in the sodalite unit to relieve ion crowding. For the same reason, four Cs^+ ions in the large cavity are found opposite 4-rings rather than at the usually preferred 6-ring sites.

During the past decade, repeated attempts to prepare fully Cs^+-exchanged zeolite A have led to gradual increases in the maximum extent of exchange, from 7/12 to 11/12.[1-5] Fully Cs^+-exchanged zeolite A, if it could be prepared (and dehydrated), would be a remarkably ionically crowded material. It is to avoid this crowding, presumably, that the zeolite does not accept 12 Cs^+ ions per 12.3 Å unit cell as the result of conventional ion-exchange procedures.[1-4] How might 12 such large ions (Cs^+, $r = 1.67$ Å[6]) be arranged in the unit cell, and what novel properties might this material have?

Two independent syntheses of Cs-A, zeolite A containing no exchangeable cations other than Cs^+, are reported here, together with their crystal structures. Two nonconventional ion-exchange methods have been employed: (1) reduction of Na^+ in dehydrated Na_{12}-A with cesium vapor, and (2) reaction of hydrated $(NH_4^+)_{12}$-A with CsOH. These reactions are driven by the following considerations, which cause the concentrations of the unwanted cations in the system to approach zero:

$$Na^+ + Cs^0 \rightarrow Na^0 + Cs^+ \quad (\Delta E°_{aq} = +0.21\ V)^7 \quad (1)$$

$$NH_4^+ + OH^- \rightarrow NH_3\uparrow + H_2O \quad (K = 5.6 \times 10^4)^8 \quad (2)$$

A single crystal[9] of Na_{12}-A (stoichiometry: $Na_{12}Si_{12}Al_{12}O_{48}\cdot 27H_2O$), 0.08 mm on an edge, was dehydrated for 48 h at 350 °C and 1.0×10^{-5} Torr, and then exposed to ca. 0.1 Torr of cesium vapor for 16 h at 345 °C. The product (crystal 1) had a black shiny surface.

For the second synthesis of Cs-A, single crystals of $(NH_4^+)_{12}$-A were prepared by flow methods.[10] They were placed in contact with an approximate 50-fold excess of wet solid cesium hydroxide for 3 h in an ultrasonic vibrator, to expedite the diffusion and loss of the NH_3 evolved. By this batch method, the number of impurity cations which the zeolite could scavenge from the exchange medium was limited.[11] One crystal was then evacuated at 24 °C and 1×10^{-5} Torr for 14 h (crystal 2, 0.08 mm on an edge). Its physical appearance was unaltered by these procedures.

The space group $Pm3m$ was used throughout this work for reasons discussed previously.[12] The structures, $a = 12.279$ (1) Å for crystal 1 and 12.291 (5) Å for crystal 2, were solved by using 201 and 87 unique reflections ($I_o > 3\sigma(I_o)$), respectively, collected on an automated diffractometer with monochromatic Mo Kα radiation. Absorption corrections (μR ca. 0.4)[13] were not applied. Other experimental details including data reduction are as previously presented.[14]

Full-matrix least-squares refinement[15] of crystal 1 using anisotropic thermal parameters for all atoms except Cs(4) quickly converged to $R_1 = \sum||F_o| - |F_c||/\sum F_o = 0.061$ and $R_2 = (\sum w(F_o - |F_c|)^2/\sum wF_o^2)^{1/2} = 0.051$. Inclusion of Cs(4) with an isotropic thermal parameter lowered these to 0.054 and 0.040, respectively, with occupancies converged at 2.99 (4), 7.01 (9), 2.18 (5), and 0.78 (12) for Cs(i), $i = 1$ to 4, and an unusually large thermal parameter for Cs(4). When the thermal parameter and occupancy of Cs(4) were free to vary, while all other occupancies were fixed,

(1) Vance, T. B., Jr.; Seff, K. *J. Phys. Chem.* **1975**, *79*, 2163-2167.
(2) Firor, R. L.; Seff, K. *J. Am. Chem. Soc.* **1977**, *99*, 6249-6253.
(3) Subramanian, V.; Seff, K. *J. Phys. Chem.* **1979**, *83*, 2166-2169.
(4) Kim, Y.; Seff, K. *Bull. Korean Chem. Soc.* **1984**, *5*, 117-121.
(5) Dejsupa, C.; Seff, K. *J. Phys. Chem.*, submitted for publication.
(6) Shannon, R. D.; Prewitt, C. T. *Acta Crystallogr., Sect. B* **1969**, *B25*, 925-946.
(7) *Handbook of Chemistry and Physics*; Chemical Rubber Co.: Cleveland, OH, 1983; 64th ed, pp D-157-158.
(8) Reference 7, p D-166.
(9) Crystals of Na_{12}-A were synthesized by Charnell's method. See Charnell, J. F. *J. Cryst. Growth* **1971**, *8*, 291-294.
(10) McCusker, L. B.; Seff, K. *J. Am. Chem. Soc.* **1981**, *103*, 3441-3446.
(11) Dejsupa, C. M.S. Thesis, University of Hawaii, 1986.
(12) Yanagida, R. Y.; Amaro, A. A.; Seff, K. *J. Phys. Chem.* **1973**, *77*, 805-809.
(13) *International Tables for X-ray Crystallography*, Vol. II; Kynoch Press: Birmingham, England, 1974; p 302.
(14) Raghavan, N. V.; Seff, K. *J. Phys. Chem.* **1976**, *80*, 2133-2137.
(15) Principle computer programs used in this study: LP76 data reduction program, Ottersen, T. University of Hawaii, 1973. Full-matrix least-squares, Gantzel, P. K.; Sparks, R. A.; Trueblood, K. N. UCLA. LS4, American Crystallographic Association Program Library (old) No. 137 (modified). Fourier program, Hubbard, C. R.; Quicksall, C. O.; Jacobson, R. A. Ames Laboratory Fast Fourier, Iowa State University, 1971.

0022-3654/87/2091-3943$01.50/0 © 1987 American Chemical Society